Scientific Research Publishing

Journal of Modern Physics, 2022, 13, 414-431
https://www.scirp.org/journal/jmp
ISSN Online: 2153-120X
ISSN Print: 2153-1196

# Ab Initio Calculation of Accurate Electronic and Transport Properties of Zinc Blende Gallium Antimonide (zb-GaSb)

**Yacouba Issa Diakite[1], Yuriy Malozovsky[2], Cheick Oumar Bamba[3], Lashounda Franklin[2], Diola Bagayoko[2]**

[1]Department of Studies and Research (DSR) in Physics, Center of Calculation, Modeling and Simulation (CCMS), College of Sciences and Techniques (CST), University of Sciences, Techniques, and Technologies of Bamako (USTTB), Bamako, Mali
[2]Department of Mathematics and Physics (DMP), Southern University and A & M College, Baton Rouge, LA, USA
[3]Louisiana State University (LSU), Baton Rouge, LA, USA
Email: yacouba_idiakite@yahoo.fr

**How to cite this paper:** Diakite, Y.I., Malozovsky, Y., Bamba, C.O., Franklin, L. and Bagayoko, D. (2022) Ab Initio Calculation of Accurate Electronic and Transport Properties of Zinc Blende Gallium Antimonide (zb-GaSb). *Journal of Modern Physics*, **13**, 414-431.
https://doi.org/10.4236/jmp.2022.134029

**Received:** February 8, 2022
**Accepted:** April 16, 2022
**Published:** April 19, 2022



## Abstract

This article reports the results of our investigations on electronic and transport properties of zinc blende gallium antimonide (zb-GaSb). Our ab-initio, self-consistent and non-relativistic calculations used a local density approximation potential (LDA) and the linear combination of atomic orbital formalism (LCAO). We have succeeded in performing a generalized minimization of the energy, using the Bagayoko, Zhao and Williams (BZW) method, to reach the ground state of the material while avoiding over-complete basis sets. Consequently, our results have the full physical content of density functional theory (DFT) and agree with available, corresponding experimental data. Using an experimental room temperature lattice constant of 6.09593Å, we obtained a direct band gap of 0.751 eV, in good agreement with room temperature measurements. Our results reproduced the experimental locations of the peaks in the total density of valence states as well as the measured electron and hole effective masses. Hence, this work points to the capability of ab-initio DFT calculations to inform and to guide the design and the fabrication of semiconductor based devices—provided a generalized minimization of the energy is performed.

## Keywords

Gallium Antimonide, BZW Method, Self-Consistent Calculation, Density Functional Theory, Band Gap

## 1. Introduction

Gallium antimonide (GaSb) is one of the semiconductor compounds of the III-V family, derived from gallium and antimony; its stable crystal structure is zinc blende. It is a direct gap semiconductor which has the possibility of being p- or n-type doped, with good mobility. It also has a significant electro-optical potential in the infrared domain [1]. GaSb has emerged in recent years as a very technologically attractive semiconductor, given its applications in high-efficiency thermo-photovoltaics, mid-infrared lasers, photodetectors, high-speed electronic devices, and non-linear optics. Such applications derive from several interesting properties of the material, such as the high hole mobility (850 - 10,800 $cm^2/Vs$), the low carrier effective masses and the small direct band gap value [2]. The importance of its technological applications makes it an extensively studied semiconductor, both theoretically and experimentally.

Table 1 shows a list of results from previous DFT and other calculations of the electronic properties of zb-GaSb. Of the ab-initio local density approximation (LDA) calculations, the first six (6) reported negative band gaps, while the next five (5) found a zero gap. The following twenty-nine (29) results obtained with an ab-initio or ad hoc LDA potential range from 0.05 eV to 1.20 eV. Ad hoc potentials have no predictive capability, as the results depend on the values of the various parameters used in their construction. The computational approaches for the calculations in the table are primarily the full potential linearized augmented plane wave (FP-LAPW). Some authors have used the projected augmented wave (PAW), Gaussian-type orbitals (GTO) or the standard pseudopotential and plane wave method. These approaches are different implementations of the linear combination of atomic orbitals (LCAO).

The calculations with ab-initio, generalized gradient approximation (GGA) potentials follow the LDA ones in the table. The resulting, calculated band gap values of zb-GaSb are not satisfactory. Indeed, of the first thirteen (13) ab-initio GGA results for the band gap, the four (4) are negative and the remaining 9 are zero. The following twenty-seven (27) results in the table, obtained with GGA ab-initio potentials, range from 0.06 eV to 1.015 eV. Five (5) of these results were obtained with the Engel and Vosko GGA which tends to overestimate band gaps. One of these results, 0.726 eV for an indirect band gap, disagrees qualitatively with experiment that reports a direct band gap.

The above ab-initio calculations are followed in the table by several calculations with ad hoc potentials. In particular, two (2) of these calculations, with an empirical pseudopotential approach, reported band gaps of 0.62 eV and 0.715 eV. Two (2) of the calculations used a version of the modified Becky and Johnson potential and eight (8) used a hybrid potential HSE06 or HSE. Five (5) calculations, with Green's function and the dressed Coulomb approximation (GWA), were not DFT calculations. Their results are between 0.51 eV and 0.85 eV, a wide range. The results of other types of ad hoc potentials such as TPSS, HISS, B3LYP and Christensen are presented in the table. We recall that the

**Table 1.** Calculated band gaps ($E_g$, in eV) of zinc blende GaSb, along with pertinent lattice constants in Angstroms, and experimental values reported in the literature.

| Computational Formalism | Potentials (DFT and others) | a (Å) | $E_g$ (eV) |
|---|---|---|---|
| PW-PP | LDA | 6.089 | −0.348 [a] |
| PW-PP | LDA | 6.043 | −0.168 [b] |
| FP-LAPW | LDA | 6.107 | −0.165 [c] |
| FP-LAPW | LDA | 6.096 | −0.13 [c] |
| Ab initio pseudopotential | LDA | | −0.10 [d] |
| FP-LAPW | LDA | | −0.09 [e] |
| FP-LMTO | LDA | 6.091 | 0.00 [f] |
| FP-LAPW + lo | LDA | | 0.00 [g] |
| FP-LAPW | LDA | 6.0619 | 0.00 [h] |
| Ab initio pseudopotential | LDA | 6.0959 | 0.00 [i] |
| Ab-initio-DFT in Plane wave | LDA | | 0.00 [j] |
| LMTO | vLB (LDA + vBL) | | 0.05 [k] |
| Hybrid exchange methodology | LSDA | | 0.09 [l] |
| PAW | LDA | 6.065 | 0.13 [m] |
| Hybrid functional method | US-LDA | | 0.23 [m] |
| NMTO | LDA | 6 | 0.25 [k] |
| Generalized density-functional theory (GDFT) | LDA | 6.12 | 0.259 [n] |
| PW-PP | LDA | 6.08 | 0.398 [o] |
| FP-LAPW | sX-LDA + SOC | | 0.43 [e] |
| LMTO | LDA | | 0.52 [k] |
| PW-PP | LDA | 5.981 | 0.547 [p] |
| Ab initio pseudopotential | LDA | 5.938 | 0.5885 [i] |
| FP-LAPW | DOS-mBJ-LDA | | 0.60 [q] |
| Sx- FLAPW | Sx-LDA | | 0.67 [r] |
| FP-LAPW + lo | mBJLDA | 6.2086 | 0.68 [s] |
| Projector-augmented-wave (PAW) | MBJLDA | | 0.73 [t] |
| Linear-muffin-tin orbital within atomic-spheres approximation (LMTO-ASA) | LDA | | 0.74 [u] |
| Projector-augmented-wave (PAW) | MBJLDA | | 0.75 [t] |
| OLCAO | LDA | | 0.80 [v] |
| FLAPW | LDA | 6.07181 | 0.80 (indirect) [w] |

**Continued**

| | | | |
|---|---|---|---|
| PW-PP (with correction) | LDA | 6.043 | 0.81 [b] |
| Projector-augmented-wave (PAW) | $MBJLDA_{bgfit}$ | | 0.82 [t] |
| FLAPW | LDA | 6.07181 | 0.82 (indirect) [w] |
| FP-LAPW + lo | mBJLDA | 6.1268 | 0.90 [s] |
| Generalized density-functional theory (GDFT) | LDA | 5.95 | 0.925 [n] |
| FP-LAPW | mBJ-LDA | | 0.94 [q] |
| NMTO | vLB | 6 | 0.94 [k] |
| FP-LAPW | mBJ-LDA | 6.0619 | 1.036 [h] |
| FLAPW | LDA | 6.07181 | 1.10 [w] |
| FP-LAPW + lo | mBJLDA | 6.0449 | 1.20 [s] |
| Projector-augmented-wave (PAW) | GGA-PBE + SOC | 6.203 | −0.477 [x] |
| Projector-augmented-wave (PAW) | GGA-PBE | 6.203 | −0.259 [x] |
| FP-LAPW | Relativistic GGA | 6.22 | −0.35 [y] |
| Projector-augmented-wave (PAW) | GGA-PBE | | −0.11 [t] |
| PAW | GGA | 6.228 | 0.00 [m] |
| Hybrid functional method | US-GGA | | 0.00 [m] |
| FP-LAPW | WC-GGA | | 0.00 [z] |
| FP-LAPW | WC-GGA | 6.107 | 0.00 [a'] |
| FP-LAPW | PBEsol-GGA | | 0.00 [h] |
| FP-LAPW + lo | WC-GGA | 6.115 | 0.00 [b'] |
| PAW | PBE | 6.237 | 0.00 [m] |
| middle-range screened hybrid exchange functional | PBE | | 0.00 [c'] |
| Projector-augmented-wave (PAW) | PBE | | 0.00 [d'] |
| middle-range screened hybrid exchange functional | $PBE_{sol}$ | | 0.06 [c'] |
| FP-LAPW + lo | GGA | | 0.07 [e'] |
| FP-LAPW | GGA-PBE | | 0.11 [r] |
| FP-LAPW | GGA | 6.09593 | 0.17 [f'] |
| PAW | GGA-PBE | 6.22 | 0.20 [g'] |
| PW-PP | GGA-PBE | 6.26 | 0.208 [o] |
| PW-PP | GGA-PW91 | 6.259 | 0.217 [o] |
| FP-LAPW | GGA-PBE | 6.2145 | 0.220 [h'] |

**Continued**

| | | | |
|---|---|---|---|
| PW-PP | GGA-RPBE | 6.26 | 0.236 [o] |
| FP-LAPW | EV-GGA | 6.1231 | 0.35 [h] |
| PW-PP | GGA-TPSS | 6.259 | 0.352 [o] |
| FP-LAPW + lo | EV-GGA | | 0.361 [g] |
| FP-LAPW + lo | EV-GGA | | 0.396 [b'] |
| FP-LAPW | GGA | 6.193 | 0.4 [i'] |
| PW-PP | GGA-PBEsol | 6.09 | 0.428 [o] |
| PW-PP | GGA-AM05 | 6.091 | 0.482 [o] |
| NMTO | PBE | 6 | 0.51 [k] |
| PW-PP | GGA-RTPSS | 6.09 | 0.513 [o] |
| Hybrid functional method | GGA HSE06 | 6.141 | 0.62 [m] |
| PW-PP | PBE-GGA | 6.06 | 0.63 [j'] |
| FP-LMTO | GGA | | 0.726 (indirect) [k'] |
| FP-LAPW | mBJ-GGA | | 0.734 [h'] |
| FP-LAPW | PBE-GGA with SOI | 6.118 | 0.812 [l'] |
| FP-LAPW | mBJ-GGA | 6.1231 | 0.844 [h] |
| FP-LAPW | non-relativistic EV-GGA | 6.24 | 1.00 [y] |
| FP-LAPW | PBE-GGA without SOI | 6.118 | 1.008 [l'] |
| PW-PP | GGA-MBJ | | 1.015 [o] |
| GW method | GW | | 0.62 [n] |
| semiempirical | LDA | 6.096 | −0.38 [m'] |
| middle-range screened hybrid exchange functional | Tao, Perdew, Staroverov and Scuseria (TPSS) Potential | | 0.09 [c'] |
| FP-LAPW and LMTO | | | 0.2 [n'] |
| middle-range screened hybrid exchange functional | Henderson, Izmaylov, Scuseria and Savin (HISS) Potential | | 0.31 [c'] |
| Projector-augmented-wave (PAW) | $GW_0$-PBE | | 0.51 [d'] |
| Projector-augmented-wave (PAW) | HSE06 + SOC | 6.124 | 0.614 [x] |
| Plane-wave pseudopotential | | | 0.54 [o'] |

**Continued**

| | | | |
|---|---|---|---|
| Projector-augmented-wave (PAW) | HSE | | 0.68 [d'] |
| middle-range screened hybrid exchange functional | HSE | | 0.70 [c'] |
| Empirical pseudopotential | Empirical pseudopotential | 6.118 | 0.715 [q'] |
| Projector-augmented-wave (PAW) | HSE06 | | 0.72 [t] |
| Hybrid exchange methodology | HSE | | 0.72 [l] |
| FP-LAPW | MBJ | | 0.763 [r'] |
| Projector-augmented-wave (PAW) | $GW^{TC\text{-}TC}$-HSE | | 0.77 [d'] |
| Projector-augmented-wave (PAW) | HSE06 | 6.124 | 0.782 [x] |
| Projector-augmented-wave (PAW) | $GWΓ^{1}$-HSE | | 0.80 [d'] |
| semiempirical | LDA + C | 6.096 | 0.81 [m'] |
| Hybrid exchange methodology | B3LYP | | 0.81 [l] |
| Projector-augmented-wave (PAW) | $HSE06_{\alpha}$ + SOC | 6.124 | 0.819 [x] |
| Projector-augmented-wave (PAW) | $HSE_{bgfit}$ | | 0.82 [t] |
| Projector-augmented-wave (PAW) | $G_0W_0{}^{TC\text{-}TC}$ | | 0.85 [t] |
| FP-LAPW | mBJ | | 0.876 [a'] |
| Projector-augmented-wave (PAW) | Christensen | | 0.88 [t] |
| | Experiment | | |
| | | 300 K | 0.67 [r'] |
| | | 300 K | 0.72 [3'] |
| | | 300 K | 0.729 [t'] |
| | | 300 K | 0.724 ± 0.005 [u'] |
| | | 300 K | 0.725 [v'] |
| | | 300 K | 0.73 [w', x'] |
| | | Room T | 0.75 [y'] |
| | | Low T | 0.78 [r'] |
| | | Low T | 0.80 [n] |
| | | Low T | 0.809 ± 0.005 [z''] |
| | | Low T | 0.81 [a''] |

**Continued**

| | | |
|---|---|---|
| | 4.2 K | 0.812 [b”] |
| | Low T | 0.82 [l] |
| | Low T | 0.822 [v’] |

[a] Ref [3], [b] Ref [4], [c] Ref [5], [d] Ref [6], [e] Ref [7], [f] Ref [8], [g] Ref [9], [h] Ref [10], [i] Ref [11], [j] Ref [12], [k] Ref [13], [l] Ref [14], [m] Ref [15], [n] Ref [16], [o] Ref [17], [p] Ref [18], [q] Ref [19], [r] Ref [20], [s] Ref [21], [t] Ref [22], [u] Ref [23], [v] Ref [24], [w] Ref [25], [x] Ref [26], [y] Ref [27], [z] Ref [28], [a’] Ref [29], [b’] Ref [30], [c’] Ref [31], [d’] Ref [32], [e’] Ref [33], [f’] Ref [34], [g’] Ref [35], [h’] Ref [36], [i’] Ref [37], [j’] Ref [38], [k’] Ref [39], [l’] Ref [40], [m’] Ref [41], [n’] Ref [42], [o’] Ref [43], [p’] Ref [44], [q’] Ref [45], [r’]Ref [46], [s’] Ref [47], [t’] Ref [48], [u’] Ref [49], [v’] Ref [50], [w’] Ref [51], [x’] Ref [52], [y’] Ref [53], [z’] Ref [54], [a”] Ref [55], [b”] Ref [56].

calculations in this paragraph, which used ad hoc DFT potentials, have no predictive capabilities.

The theoretical results discussed above and shown in **Table 1** disagree with each other and with the experimental values of the band gap. Seven (7) of these experimental values, in the last 14 rows of **Table 1**, range from 0.67 eV to 0.75 eV, for eight (8) measurements at room temperature; and seven (7) other values are from 0.78 eV to 0.822 eV for low temperature experiments. The apparent, experimental agreement on a band gap around 0.81 eV, for low temperatures, and around 0.73 eV, for room temperature, contrasts strongly with the case of theoretical studies with 24 negative values or zero for the band gap of zb-GaSb. The disagreement between the theoretical values of the ab-initio DFT calculations and between these values and the accepted experimental values is the main motivation for this work. The importance of a correct, calculated band gap resides in the need to produce accurate optical and dielectric properties, densities of states, and effective masses. These quantities, among others, cannot be correctly calculated using an incorrect, theoretical band gap.

Our motivation to resolve the discrepancies noted above is further supported by the fact that the previous works of our group accurately described or predicted properties of semiconductors, using ab-initio DFT potentials [57] [58]. This feat was made possible by our use of the Bagayoko, Zhao and Williams (BZW) method or its enhancement by Ekuma and Franklin (BZW-EF). Bagayoko explained that these methods seek out and reach the ground state of a material without using over-completes basis sets. To our knowledge, none of the calculations in **Table 1** used successive, self-consistent calculations, with increasingly large, augmented basis sets, to reach verifiably the ground state of the material. The attainment of the ground state is required by the second DFT theorem and is essential for the results of a DFT calculation to have the full, physical content of DFT and to be consistent with experiment [57].

After this introduction, focused on the importance of the material and the previous theoretical and experimental studies, we describe in Section 2 our method of calculation and the details relating to the replication of our work. Section

3 is devoted to the presentation and discussion of our results for the band structure and the band gap, as well as the total and partial densities of states, and the effective masses of electrons and holes. A relatively succinct conclusion is set out in Section 4.

## 2. Computational Method

We used in this work the local density approximation (LDA) potential of Ceperley and Alder [59], as parameterized by Vosko, Wilk and Nusair [60]. We have applied the linear combination of atomic orbitals. Gaussian functions constitute the radial parts of these orbitals. We used a software package that was developed and refined over a decade at the US Department of Energy's Ames Laboratory, Ames, Iowa [61]. Our non-relativistic calculations utilized an experimental lattice constant, at room temperature. We applied the BZW method to perform the linear combination of atomic orbitals (LCAO). Our method allows the concomitant and self-consistent solution of the two coupled equations. The first is that of Kohn and Sham [62] while the second equation generates the density of charge—using only the wave functions of the occupied states. The second equation can be considered as a constraint on the Kohn-Sham equation (KS). Many other details on the BZW or BZW-EF method are widely explained in the previous articles [57] [63]-[69]. We describe the generalized minimization of the energy below.

Briefly, our approach uses successive and consistent computations, with basis augmented sets to perform a generalized energy minimization, as required by the second DFT theorem. If two consecutive calculations lead to the same occupied energies, these energies are local minimum the next, consecutive calculations lowers some of the occupied energies. However, if the third calculation produces the same occupied energies as the previous two, then these occupied energies have reached their absolute minima, in other words, the ground state. The necessary and sufficient criterion for stopping the computation is to have three consecutive calculations that produce identical, occupied energies.

In accordance with the above, our calculations necessarily begin with a small basis set which accommodate all the electrons of the system under study. Calculation II follows, with a basis set comprising that of Calculation I plus an orbital representing an excited state. We compare the occupied energies of the two self-consistent calculations: invariably, some occupied energies from calculation II are lower than their corresponding values from calculation I. We augment the basis set of calculation II, with an orbital, to perform calculation III. We compare the occupied energies from calculations II and III. We continue this process until three consecutive calculations produce the same occupied energies, indicating that we reached the ground state. Among these three (3) consecutive calculations, only the first, which has the smallest basis set, provides the DFT description of the ground state of the material [57] [58] [63]-[69]. The basis set of this calculation is the optimal basis set. The optimal basis set, once self-consistent

is achieved, leads to the ground state charge density of the material. Likewise, basis sets which are larger than the optima one, and which contain the optimal one, lead to the ground state charge density upon reaching self-consistency. As explained by our group in the publications referenced above and others, the use of these larger basis sets also lowers certain unoccupied energies: these lowered unoccupied energies are not due to a physical interaction in the Hamiltonian which has not changed from its value obtained with the optimal basis set. Incidentally, since the occupied energies do not change once, we reach the optimal basis set, the further lowering of some unoccupied energies because of using larger basis sets containing the optimum is one plausible explanation of the almost universal underestimation of band gaps and energy gaps by mainstream calculations [70]. Indeed, these calculations, to date, have used a single basis set which was deliberately chosen to be large in order to ensure completeness. Most often, these basis sets were over-complete for the description of the ground state [57].

Details relevant to the replication of our work follow. The crystal structure of GaSb is Zinc Blende [1]. We have used a measured value of the lattice constant at room temperature, 6.09593 Å. The self-consistent calculations for $Ga^{3+}$ and $Sb^{2-}$ provided the orbitals for the solid-state calculations. Gaussian functions are in the radial parts of atomic wave functions. We employed a set of even-tempered Gaussian exponents, with a minimum of 0.148 and a maximum of $0.93061 \times 10^5$ in atomic units, for $Ga^{3+}$. Nineteen (19) Gaussian functions were used for s and p orbitals, and 17 for d orbitals. Likewise, to describe $Sb^{3-}$, the exponents in Gaussian functions ranged from 0.125 to a maximum of $0.8 \times 10^5$. The numbers of Gaussian functions for s and p orbitals are 22 and that of the d orbitals is 19. A mesh 60 k points, with appropriate weights in the irreducible Brillouin zone, was used in the iterations for self-consistency. The error in calculating the valence charge was −0.0027647 for 44 electrons, or $-6.28 \times 10^{-5}$ per electron. The convergence criterion of the iterations is to have a difference not greater than $10^{-5}$ between the values of the potentials for two consecutive iterations. The number of iterations for this convergence was around 60. With the method described above and the associated calculation details, we studied zb-GaSb as presented below.

## 3. Results and Discussions

We present the successive calculations in **Table 2**. Columns 1, 2 and 3 of the table indicate respectively the number of a calculation, the valence state orbitals for $Ga^{3+}$ and the valence state orbitals for $Sb^{3-}$. Columns 4 and 5 show the total number of valence functions and the direct band gap calculated at the Γ point, respectively. In this table, the occupied energies from calculations IV, V and VI are identical, within our calculation uncertainty of 5 meV. Therefore, Calculation IV provides the DFT description of zb-GaSb, in accordance with the above description of our method. In particular, the occupied energies from this

**Table 2.** The successive, self-consistent calculations of the BZW method for zb-GaSb.

| Calculation number | Trial function for valence states of $Ga^{+3}$ | Trial function for valence states of $Sb^{-3}$ | No. of functions | Band Gap at Γ (in eV) |
|---|---|---|---|---|
| I | $3s^2 3p^6 3d^{10} 4s^2 4p^0$ | $4s^2 4p^6 4d^{10} 5s^2 5p^4$ | 52 | 1.629 |
| II | $3s^2 3p^6 3d^{10} 4s^2 4p^0 5s^0$ | $4s^2 4p^6 4d^{10} 5s^2 5p^4$ | 54 | 0.564 |
| III | $3s^2 3p^6 3d^{10} 4s^2 4p^0 5s^0 4d^0$ | $4s^2 4p^6 4d^{10} 5s^2 5p^4$ | 64 | 0.421 |
| **IV** | **$3s^2 3p^6 3d^{10} 4s^2 4p^0 5s^0 4d^0 5p^0$** | **$4s^2 4p^6 4d^{10} 5s^2 5p^4$** | **70** | **0.751** |
| V | $3s^2 3p^6 3d^{10} 4s^2 4p^0 5s^0 4d^0 5p^0 5d^0$ | $4s^2 4p^6 4d^{10} 5s^2 5p^4$ | 80 | 0.795 |
| VI | $3s^2 3p^6 3d^{10} 4s^2 4p^0 5s^0 4d^0 5p^0 5d^0 6s^0$ | $4s^2 4p^6 4d^{10} 5s^2 5p^4$ | 82 | 0.644 |

calculation are those for the ground state of the material. The resulting charge density is that of the ground state of zb-GaSb.

We show in Figure 1 the calculated electronic energy band structure of zb-GaSb, from calculation IV. The direct band gap calculated at the Γ point is 0.751 eV. This value is in excellent agreement with the experimental value of 0.75 eV, at room temperature 0.75 eV [53].

Various characteristics of the electronic band structure can be explained in more detail using the table of calculated eigenvalues at high points symmetry in the Brillouin zone and figures for the total and partial densities states. Figure 2 and Figure 3 show the total state density (DOS) and the partial densities of state (pDOS), respectively, as derived from the bands in Figure 1. Many parts of our calculated density of state are very close to corresponding experimental values obtained by X-ray photoemission spectroscopy measurements [71]. Figure 14 of the paper of Ley *et al.* [71] reported the peak positions of HIT, I2, I1, S1, HIB, PII, HIIIT and PIII, respectively, at −0.8 eV, −1.7 eV, −2.1 eV, −3.4 eV, −3.7 eV, −6.4 eV, −9.2 eV and −10.0 eV. According to our work, the corresponding values are respectively −0.675 eV, −1.611 eV, −2.080 eV, −3.192 eV, −3.661 eV, −6.354 eV, −9.165 eV, and −9.809 eV. While the widths of the different groups of valence bands can be extracted from the total density of states, they are more easily derived from the contents of Table 3 which shows the calculated eigenvalues at high symmetry points in the Brillouin zone.

The total valence band width is 15.862 eV. The width of the lowest laying group of bands is 0.106 eV. The widths of the middle and upper most groups valence bands are respectively 2.651 eV and 6.847 eV. These widths, derived from Table 3, can also be estimated using the content of the figure below for TDOS. A purpose of this table is to be able to make comparisons with possible future experimental measurements of X-ray, ultraviolet (UV) or other spectroscopy.

According to our calculated pDOS in Figure 3, the lowest lying group of valence bands comes almost entirely from Ga d. The middle group of valence bands is largely from Sb s, with a small contribution from Ga s. The upper most group of valence bands is unmistakably dominated by Sb p, Ga p, and Ga s, with a very small contribution of Sb s.

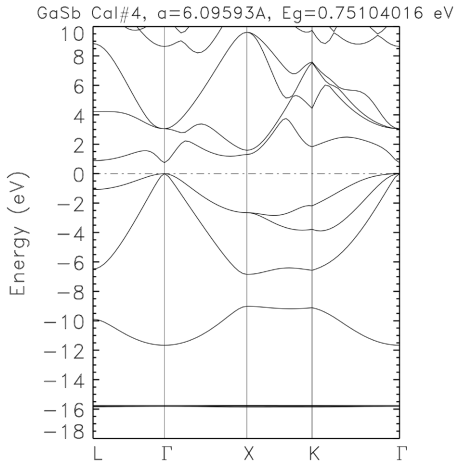


**Figure 1.** Calculated, band structure of zinc blende gallium antimonide (zb-GaSb), as obtained by the BZW method from Calculations IV. The calculated direct band gap is 0.751 eV.

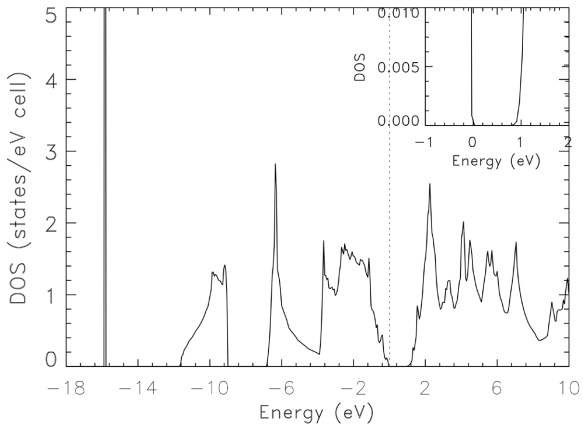


**Figure 2.** The calculated, total density of states of zb-GaSb, obtained from the energy bands in **Figure 1**. The zero on the horizontal axis indicates the position of the Fermi level.

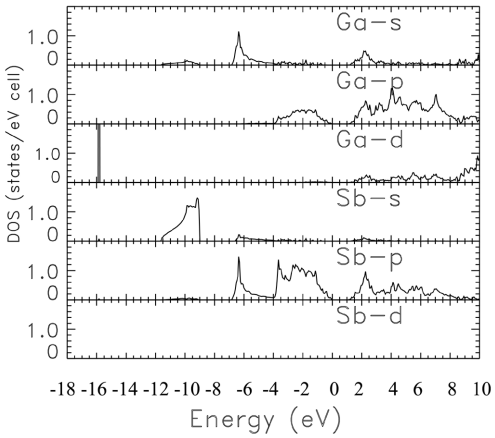


**Figure 3.** Calculated, partial densities of states (pDOS) for zb-GaSb, as derived from the bands in **Figure 1**. The zero on the horizontal axis indicates the position of the Fermi level.

**Table 3.** Calculated, electronic energies of zb-GaSb at high symmetry points in the Brillouin Zone, as obtained with the optimal basis set of Calculation IV. We used the experimental lattice constant of 6.09593 Å. This table is partly to enable comparisons with future room temperature, experimental and theoretical results.

| L-point | Γ-point | X-point | K-point |
|---|---|---|---|
| 8.836 | 3.053 | 9.612 | 7.590 |
| 4.221 | 3.053 | 9.612 | 7.556 |
| 4.221 | 3.053 | 1.591 | 4.436 |
| 0.885 | 0.751 | 1.302 | 1.827 |
| −1.080 | 0.000 | −2.651 | −2.187 |
| −1.080 | 0.000 | −2.651 | −3.785 |
| −6.480 | 0.000 | −6.847 | −6.568 |
| −9.894 | −11.665 | −9.014 | −9.110 |
| −15.759 | −15.759 | −15.756 | −15.758 |
| −15.759 | −15.759 | −15.767 | −15.764 |
| −15.814 | −15.824 | −15.803 | −15.805 |
| −15.814 | −15.824 | −15.803 | −15.806 |
| −15.850 | −15.824 | −15.862 | −15.861 |

We used the electron band structure from Calculation IV (in **Figure 1**) to calculate the effective masses of the electron, at the bottom of the conduction band, and of the holes, at the top of the valence band. We present our results, as well as other theoretical and experimental values, in **Table 4**. The effective masses of the electrons are indicated by me while those of the heavy and light holes are respectively noted as $m_{hh}$ and $m_{lh}$. The first column shows the effective masses with the specific directions in which they are calculated. It is gratifying to note that our calculated effective masses are in general agreement with experience [55] [74] [75] [76], and with parts of some previously calculated ones [12] [26] [72] [73]. Out of the nine (9) effective masses in **Table 4**, the only one for which there is a difference between an experimental value and our result is $m_{hh}$ (Γ-L) for which we found 0.682 $m_0$ while the experiments report from 0.24 $m_0$ to 0.59 $m_0$ [74] [75] [76].

For Reference [a], atheo and aexp indicate results obtained with a theoretical and an experimental lattice constant.

The above agreement between our calculated effective masses and the corresponding, experimental values indicates the correct rendering, by our calculations, of the curvatures of the bands at the conduction band minimum (CBM) and the valence band maximum (VBM).

A discussion of our results, compared to previous ones, follows. We first recall that our main motivation for this work was the resolution of the glaring disagreement between measured band gaps of approximately 0.81 eV and 0.73 eV,

**Table 4.** Calculated, effective masses for zb-GaSb (in units of the free electron-mass, $m_0$): $m_e$ indicates an electron effective mass at the bottom of the conduction band; $m_{hh}$, and $m_{lh}$ represent the heavy and light hole effective masses, respectively. Theo.: theory, expt.: experiment.

| | Our work | Theo. $a_{theo}$ [a] | Theo. $a_{exp}$ [a] | Theo. [b] | Theo. [c] | Theo. [d] | Expt. [e] | Expt. [f] | Expt. [g] | Expt. [h] |
|---|---|---|---|---|---|---|---|---|---|---|
| $m_e$ (Γ-L) | 0.041 | 0.036 | 0.008 | | 0.045 | 0.045 | | | | |
| $m_e$ (Γ-X) | 0.041 | 0.035 | 0.004 | | 0.045 | | 0.039 average | 0.042 ± 0.001 average | | 0.039 ± 0.001 average |
| $m_e$ (Γ-K) | 0.040 | 0.035 | 0.006 | | 0.045 | | | | | |
| $m_{hh}$ (Γ-L) | 0.682 | 0.646 | 0.747 | 0.551 | 0.710 | 0.55 | | 0.40 ± 0.16 | 0.36 ±0.03 | 0.44 ± 0.15 |
| $m_{hh}$ (Γ-X) | 0.280 | 0.272 | 0.219 | 0.231 | 0.247 | 0.38 | 0.250 | 0.29 ±0.09 | 0.26 ± 0.04 | |
| $m_{hh}$ (Γ-K) | 0.397 | 2.074 | 2.274 | | 0.500 | 0.45 | | 0.36 ± 0.13 | 0.38 ± 0.04 | |
| $m_{lh}$ (Γ-L) | 0.035 | 0.030 | 0.008 | 0.047 | 0.045 | | | | 0.052 ± 0.004 | |
| $m_{lh}$ (Γ-X) | 0.036 | 0.035 | 0.004 | 0.052 | 0.051 | 0.049 | 0.044 | 0.042 ± 0.002 | 0.052 ± 0.005 | 0.038 ± 0.002 |
| $m_{lh}$ (Γ-K) | 0.038 | 0.031 | 0.006 | | 0.046 | | | | 0.052 ± 0.004 | |

[a] Ref [11], [b] Ref [72], [c] Ref [26], [d] Ref [73], [e] Ref [55], [f] Ref [74], [g] Ref [75], [h] Ref [76].

for low and room temperatures, respectively, and the results of dozens of ab-initio theoretical studies that have consistently underestimated them. In particular, 24 LDA or GGA ab-initio studies reported negative numbers or zero for the bandgap of zb-GaSb. The section describing our method points to a reason that previous, ab-initio DFT calculations generally underestimated the measured values: none of these calculations performed a generalized minimization of the energy to reach the ground state in a verifiable way, as required by the second DFT theorem. Therefore, while the output of such a calculation is self-consistent, it is a stationary state among an infinite number of such states. There is an infinite number of basis sets which can lead to self-consistent (*i.e.*, stationary) results. Therefore, the chances for a single basis set calculation to produce the ground state energies while avoiding over-complete basis sets are practically zero. On the other hand, our calculations have explicitly reached the ground state and avoided the use of over-complete basis sets.

Our results, due to our strict adherence to the conditions of validity of the DFT, have the entire physical content of the DFT. They agree with the available, corresponding, experimental data, as was the case for the band gap at room temperature (*i.e.*, 0.75 eV). Our work also made it possible to obtain the experimentally identified locations of the peaks in the total density of valence states.; This agreement points to the overall correct description of the ground state band structure by our calculations. In addition, this overall description of the bands is further indicated by our correct rendering of noted curvatures of the bands, in accordance with our results for the effective masses.

The results of Reference 12 for the electron effective masses confirmed our contention that as the bottom of the conduction band is spuriously lowered,

when using over-complete basis sets, the calculated electron effective masses fall below the corresponding, experimental ones. With band gap of 0.588 eV, these authors [12] found electron effective masses of 0.036, 0.035, and 0.035 $m_0$; for the much smaller band gap of zero, these electron effective masses are respectively 0.008, 0.004, and 0.006 $m_0$. Both sets of values are lower than the corresponding ones from our calculation.

Our truly ground state calculations [57] did not need to invoke self-interaction correction of the derivative discontinuity of the exchange correlation energy in order for their outcomes to agree with available, corresponding, experimental ones. The same was true for several previous works of our group [57] [58] [63]-[69].

## 4. Conclusion

We have performed ab initio, self-consistent calculations of electronic energy bands, total and partial densities of states and of effective masses for zb-GaSb. With the method of Bagayoko, Zhao and Williams (BZW), we performed a generalized minimization of the energy to reach the ground state, verifiably, without using over-complete basis sets. Our work reproduced not just the correct, experimental room temperature band gap, but also the locations of the peaks in the total density of states, and the electron and holes effective masses. With this overall accuracy, our calculated results can inform and guide the design and fabrication of semiconductor based devices, as envisioned by the Materials Genome Initiatives (MGI).

## Acknowledgements

Our work was funded in part by the US Fulbright Fellowship Program, the Malian Ministry of Higher Education and Scientific Research, The US National Science Foundation (NSF Award No. HRD-2009765), the Louisiana Optical Network Initiative (LONI), at Southern University and A & M College in Baton Rouge (SUBR), and LaSPACE.

## Conflicts of Interest

The authors declare no conflicts of interest regarding the publication of this paper.

## References

[1] Majeed, S. and Al-Rawi, B.K. (2021) *IOP Conference Series*: *Materials Science and Engineering*, **1095**, Article ID: 012003. https://doi.org/10.1088/1757-899X/1095/1/012003

[2] Samajdar, D.P., Das, U., Sharma, A.S., Das, S. and Dhar, S. (2016) *Current Applied Physics*, **16**, 1687-1694. https://doi.org/10.1016/j.cap.2016.10.010

[3] Wang, J.W., Zhang, Y. and Wang, L.-W. (2015) *Physical Review B*, **92**, Article ID: 045211.

[4] Wang, J.W. and Zhang, Y. (2014) *Journal of Applied Physics*, **116**, Article ID:

214301. https://doi.org/10.1063/1.4903063

[5] Wei, S.-H. and Zunger, A. (1989) *Physical Review B*, **39**, 3279-3304. https://doi.org/10.1103/PhysRevB.39.3279

[6] Zhu, X.J. and Louie, S.G. (1991) *Physical Review B*, **43**, 14142-14156. https://doi.org/10.1103/PhysRevB.43.14142

[7] Rhim, S.H., Kim, M. and Freeman, A.J. (2005) *Physical Review B*, **71**, Article ID: 045202. https://doi.org/10.1103/PhysRevB.71.045202

[8] Caid, M. and Rached, D. (2020) *Materials Science-Poland*, **38**, 320-327. https://doi.org/10.2478/msp-2020-0027

[9] Ahmed, R., Fazal-E-Aleem, Hashemifar, S.J., Rashid, H. and Akbarzadeh, H. (2009) *Communications in Theoretical Physics*, **52**, 527. https://doi.org/10.1088/0253-6102/52/3/28

[10] Hadjab, M., Bennacer, H., Berrah, S., Abid, H. and Ziane, I.M. (2015) Density Functional Approach to Study Structural and Electronic Properties of III-Sb Semiconductors by Modified Becke-Johnson Potential. In: *The First National Conference on Electronics and New Technologies* (*NCENT*'2015), May 19-20, M'Sila, 1-4.

[11] Karazhanov, S.Zh. and Lew Yan Voon, L.C. (2005) Ab Initio Studies of the Band Parameters of III-V and II-VI Zinc-Blende Semiconductors. *Semiconductors*, **39**, 161-173. https://doi.org/10.1134/1.1864192

[12] Johnson, K.A. and Ashcroft, N.W. (1998) *Physical Review B*, **58**, 15548-15556. https://doi.org/10.1103/PhysRevB.58.15548

[13] Datta, S., Singh, P., Chaudhuri, C.B., Jana, D., Harbola, M.K., Johnson, D.D. and Mookerjee, A. (2019) Simple Correction to Bandgap Problems in IV and III-V Semiconductors: An Improved, Local First-Principles Density Functional Theory. https://lib.dr.iastate.edu/mse_pubs/301

[14] Tomic, S., Montanari, B. and Harrison, N.M. (2008) *Physica E*, **40**, 2125-2127. https://doi.org/10.1016/j.physe.2007.10.022

[15] Bakulin, A.V. and Kulkova, S.E. (2014) *Russian Physics Journal*, **57**, 996-999. https://doi.org/10.1007/s11182-014-0336-1

[16] Remediakis, I.N. and Kaxira, E. (1999) *Physical Review B*, **59**, 5536. https://doi.org/10.1103/PhysRevB.59.5536

[17] Castano-Gonzalez, E.E., Sena, N., Mendoza-Estrada, V., Gonzalez-Hernandez, R., Dussan, A. and Mesa, F. (2016) *Semiconductors*, **50**, 1280-1286. https://doi.org/10.1134/S1063782616100110

[18] Wang, S.Q. and Ye, H.Q. (2002) *Physical Review B*, **66**, 235111-235118.

[19] Singh, A.K., Chandra, D., Kattayat, S., Kumar, S., Alvi, P.A. and Rathi, A. (2019) *Semiconductors*, **53**, 1584-1592. https://doi.org/10.1134/S1063782619160267

[20] Geller, C.B., Wolf, W., Picozzi, S., Continenza, A., Asahi, R., Mannstadt, W., Freeman, A.J. and Wimmer, E. (2001) *Applied Physics Letters*, **79**, 368. https://doi.org/10.1063/1.1383282

[21] Camargo-Martinez, J.A. and Baquero, R. (2012) *Physical Review B*, **86**, Article ID: 195106. https://doi.org/10.1103/PhysRevB.86.195106

[22] Kim, Y.-S., Marsman, M. and Kresse, G. (2010) *Physical Review B*, **82**, Article ID: 205212. https://doi.org/10.1103/PhysRevB.82.205212

[23] Puska, M.J., Lanki, P. and Nieminen, R.M. (1989) *Journal of Physics*: *Condensed Matter*, **1**, 6081. https://doi.org/10.1088/0953-8984/1/35/008

[24] Huang, M.Z. and Ching, W.Y. (1993) *Physical Review B*, **47**, 9449.

https://doi.org/10.1103/PhysRevB.47.9449

[25] Khanin, D.V. and Kul'kova, S.E. (2005) *Russian Physics Journal*, **48**, 70-77. https://doi.org/10.1007/s11182-005-0086-1

[26] Bastos, C.M.O., Sabino, F.P., Sipahi, G.M. and Da Silva, J.L.F. (2018) *Journal of Applied Physics*, **123**, Article ID: 065702. https://doi.org/10.1063/1.5018325

[27] Briki, M., Abdelouhab, M., Zaoui, A. and Ferhat, M. (2009) *Superlattices and Microstructures*, **45**, 80-90. https://doi.org/10.1016/j.spmi.2008.12.022

[28] Hassan, F.E. and Postnikov, A.V. (2010) *Journal of Alloys and Compounds*, **504**, 559. https://doi.org/10.1016/j.jallcom.2010.05.161

[29] Oumelaz, F., Nemiri, O., Boumaza, A., Ghemid, S., Meradji, H., Bin Omran, S., El Haj Hassan, F., Rai, D.P. and Khenata, R. (2017) *Indian Journal of Physics*, **92**, 705-714. https://doi.org/10.1007/s12648-017-1157-1

[30] El Haj Hassan, F., Breidi, A., Ghemid, S., Amrani, B., Meradji, H. and Pages, O. (2010) *Journal of Alloys and Compounds*, **499**, 80-89. https://doi.org/10.1016/j.jallcom.2010.02.121

[31] Lucero, M.J., Henderson, T.M. and Scuseria, G.E. (2012) *Journal of Physics*: *Condensed Matter*, **24**, Article ID: 145504. https://doi.org/10.1088/0953-8984/24/14/145504

[32] Hinuma, Y., Gruneis, A., Kresse, G. and Oba, F. (2014) *Physical Review B*, **90**, Article ID: 155405. https://doi.org/10.1103/PhysRevB.90.155405

[33] Drablia, S., Meradji, H., Ghemid, S., Labidi, S. and Bouhafs, B. (2009) *Physica Scripta*, **79**, Article ID: 045002. https://doi.org/10.1088/0031-8949/79/04/045002

[34] Malsawmtluanga, A., Lalnunpuia, Ralte, R.L. and Pachuau, Z. (2014) *Indian Journal of Scientific Research and Technology*, **2**, 108-111.

[35] Tahini, H.A., Chroneos, A., Murphy, S.T., Schwingenschogl, U. and Grimes, R.W. (2013) *Journal of Applied Physics*, **114**, Article ID: 063517. https://doi.org/10.1063/1.4818484

[36] Salehi, H., Badehian, H.A. and Farbod, M. (2014) *Materials Science in Semiconductor Processing*, **26**, 477-490. https://doi.org/10.1016/j.mssp.2014.05.020

[37] Al-Douri, Y. and Reshak, A. (2011) *Applied Physics A*, **104**, 1159-1167. https://doi.org/10.1007/s00339-011-6400-6

[38] Othman, M.S.H., Mishjil, K.A. and Habubi, N.F. (2012) *Chinese Physics Letters*, **29**, Article ID: 037302.

[39] Benaline Sheeba, V. and Louis, C.N. (2016) *International Journal of Scientific Research and Innovations*, **1**, 1-5.

[40] Ali, M.A., Aleem, H., Sarwar, B. and Murtaza, G. (2020) *Indian Journal of Physics*, **94**, 477-484.

[41] Wei, S.-H., Nie, X.L., Batyrev, I.G. and Zhang, S.B. (2003) *Physical Review B*, **67**, Article ID: 165209. https://doi.org/10.1103/PhysRevB.67.165209

[42] Reshak, A.H. (2005) *The European Physical Journal B*, **47**, 503-508. https://doi.org/10.1140/epjb/e2005-00364-3

[43] Wang, S.Q. and Ye, H.Q. (2002) *Journal of Physics*: *Condensed Matter*, **14**, 9579-9587. https://doi.org/10.1088/0953-8984/14/41/313

[44] Bouerissa, N., Baaziz, H. and Charifi, Z. (2002) *Physica Status Solidi* (*b*), **231**, 403-410. https://doi.org/10.1002/1521-3951(200206)231:2<403::AID-PSSB403>3.0.CO;2-6

[45] Gazhulina, A.P. and Maryche, M.O. (2015) *Journal of Alloys and Compounds*, **623**, 413. https://doi.org/10.1016/j.jallcom.2014.11.028

[46] Lide, D.R. (2004) CRC Handbook of Chemistry and Physics: A Ready-Reference Book of Chemical and Physical Data. CRC Press, Boca Raton.

[47] Adachi, S. (1987) *Journal of Applied Physics*, **61**, 4869. https://doi.org/10.1063/1.338352

[48] Iyer, S., Hegde, S., Abul-Fadl, A., Bajaj, K.K. and Mitchel, W. (1993) *Physical Review B*, **47**, 1329-1339. https://doi.org/10.1103/PhysRevB.47.1329

[49] Munoz, M., Wei, K. and Pollak, F.H. (1999) *Physical Review B*, **60**, 8105-8110. https://doi.org/10.1103/PhysRevB.60.8105

[50] Dutta, P.S. and Bhat, H.L. (1997) *Journal of Applied Physics*, **81**, 5821. https://doi.org/10.1063/1.365356

[51] Vladimir, A. and Serget, R. (2002) *Physical Status Solidi* (*b*), **244**, 243-248.

[52] Steiner, T.D. (2004) Semiconductor Nanostructures for Optoelectronic Applications. Artech House, Boston. https://doi.org/10.1108/sr.2004.24.3.320.3

[53] Arévalo, F., Saavedra, R. and Paulraj, M. (2008) *Journal of Physics*: *Conference Series*, **134**, Article ID: 012019. https://doi.org/10.1088/1742-6596/134/1/012019

[54] Munoz, M. and Pollak, F.H. (2000) *Physical Review B*, **62**, 16600-16604.

[55] Vurgaftman, I., Meyer, J.R. and Ram-Mohan, L.R. (2001) *Journal of Applied Physics*, **89**, 5815. https://doi.org/10.1063/1.1368156

[56] Dutta, P.S., Koteswara Rao, K.S.R., Bhat, H.L. and Kumar, V. (1995) *Applied Physics A*, **61**, 149-152. https://doi.org/10.1007/BF01538381

[57] Bagayoko, D. (2014) *AIP Advances*, **4**, Article ID: 127104. https://doi.org/10.1063/1.4903408

[58] Diakite, Y.I., Traore, S.D., Malozovsky, Y., Khamala, B., Franklin, L. and Bagayoko, D. (2017) *Journal of Modern Physics*, **8**, 531-546. https://doi.org/10.4236/jmp.2017.84035

[59] Ceperley, D.M. and Alder, B.J. (1980) *Physical Review Letters*, **45**, 566. https://doi.org/10.1103/PhysRevLett.45.566

[60] Vosko, S.H., Wilk, L. and Nusair Can, M. (1980) *Canadian Journal of Physics*, **58**, 1200-1211. https://doi.org/10.1139/p80-159

[61] Harmon, B.N., Weber, W. and Hamann, D.R. (1982) *Physical Review B*, **25**, 1109-1115. https://doi.org/10.1103/PhysRevB.25.1109

[62] Kohn, W. and Sham, L.J. (1965) *Physical Review*, **140**, A1133-A1138. https://doi.org/10.1103/PhysRev.140.A1133

[63] Bagayoko, D, Zhao, G.L., Fan, J.D. and Wang, J.T. (1998) *Journal of Physics*: *Condensed Matter*, **10**, 5645-5655. https://doi.org/10.1088/0953-8984/10/25/014

[64] Zhao, G.L., Bagayoko, D. and Williams, T.D. (1999) *Physical Review B*, **60**, 1563. https://doi.org/10.1103/PhysRevB.60.1563

[65] Ekuma, C.E., Jarrell, M., Moreno, J. and Bagayoko, D. (2013) *Physics Letters A*, **377**, 2172-2176. https://doi.org/10.1016/j.physleta.2013.05.043

[66] Franklin, L., Ekuma, C.E., Zhao, G.L. and Bagayoko, D. (2013) *Journal of Physics and Chemistry of Solids*, **74**, 729-736. https://doi.org/10.1016/j.jpcs.2013.01.013

[67] Bagayoko, D. and Franklin, L. (2005) *Journal of Applied Physics*, **97**, Article ID: 123708. https://doi.org/10.1063/1.1939069

[68] Diakite, Y.I., Traoré, S.D., Malozovsky, Y., Khamala, B., Franklin, L. and Bagayoko, D. (2015) *The African Review of Physics*, **10**, 315-327.

[69] Bamba, C.O., Inakpenu, R., Diakite, Y.I., Franklin, L., Malozovsky, Y., Stewart, A.D.

and Bagayoko, D. (2017) *Journal of Modern Physics*, **8**, 1938-1949. https://doi.org/10.4236/jmp.2017.812116

[70] Bagayoko, D. (1983) *International Journal of Quantum Chemistry*, **17**, 527.

[71] Ley, L., Pollak, R.A., McFeely, F.R., Kowalczyk, S.P. and Shirley, D.A. (1974) *Physical Review B*, **9**, 600-621. https://doi.org/10.1103/PhysRevB.9.600

[72] Huang, M.Z. and Ching, W.Y. (1985) *Journal of Physics and Chemistry of Solids*, **46**, 977. https://doi.org/10.1016/0022-3697(85)90101-5

[73] Higginbothan, C.W., Pollak, F.H. and Cardona, M. (1968) Band Structure and Optical Constants of InSb, InAs, and GaSb: The k.p Method. *Proceeding of IX International Conference on the Physics of Semiconductors*, Moscow, Vol. 1, 57.

[74] Reine, M., Aggarwal, R.L. and Lax, B. (1972) *Physical Review B*, **5**, 3033-3049. https://doi.org/10.1103/PhysRevB.5.3033

[75] Stradling, R.A. (1966) *Physics Letters*, **20**, 217-218. https://doi.org/10.1016/0031-9163(66)90330-1

[76] Filion, A. and Fortin, E. (1973) *Physical Review B*, **8**, 3852-3860. https://doi.org/10.1103/PhysRevB.8.3852